Assembly and Test of SQ01b, a Nb_3Sn Quadrupole Magnet for the LHC Accelerator Research Program

P. Ferracin, G. Ambrosio, S. E. Bartlett, B. Bordini, R. H. Carcagno, S. Caspi, D. R. Dietderich, S. Feher, S. A. Gourlay, A. R. Hafalia, V. V. Kashikhin, M. J. Lamm, A. F. Lietzke, S. Mattafirri, A. D. McInturff, D. F. Orris, Y. M. Pischalnikov, G. L. Sabbi, C. D. Sylvester, M. A. Tartaglia, G. V. Velev, and A. V. Zlobin

***Abstract*—The US LHC Accelerator Research Program (LARP) consists of four US laboratories (BNL, FNAL, LBNL, and SLAC) collaborating with CERN to achieve a successful commissioning of the LHC and to develop the next generation of Interaction Region magnets. In 2004, a large aperture Nb_3Sn racetrack quadrupole magnet (SQ01) has been fabricated and tested at LBNL. The magnet utilized four subscale racetrack coils and was instrumented with strain gauges on the support structure and directly over the coil's turns. SQ01 exhibited training quenches in two of the four coils and reached a peak field in the conductor of 10.4 T at a current of 10.6 kA. After the test, the magnet was disassembled, inspected with pressure indicating films, and reassembled with minor modifications. A second test (SQ01b) was performed at FNAL and included training studies, strain gauge measurements and magnetic measurements. Magnet inspection, test results, and magnetic measurements are reported and discussed, and a comparison between strain gauge measurements and 3D finite element computations is presented.**

***Index Terms*—LARP, Nb_3Sn, quadrupole magnet**

I. Introduction

As part of the LHC Accelerator Research Program (LARP [1], [2]), three US national laboratories (BNL, FNAL, and LBNL) are currently engaged in the development of superconducting magnets for the LHC Interaction Regions (IR) beyond the current design [3], [4]. In 2004, LBNL fabricated, assembled, and tested SQ01, a Nb_3Sn quadrupole magnet implementing four "subscale" racetrack coils, whose main goal was providing a cost effective tool for technology development studies. After the test at LBNL, reported in [5], the magnet was disassembled, inspected and reassembled. In January 2005, a second test was performed at FNAL, as part of the LARP Supporting R&D effort. In this paper we briefly outline the main inspection outcomes, and we present the results of the second test, which included quench performance, temperature and ramp-rate dependence studies, as well as magnetic and strain gauge measurement [6].

Manuscript received September 20, 2005. This was supported by the Director, Office of Energy Research, Office of High Energy and Nuclear Physics, High Energy Physics Division, U. S. Department of Energy, under Contract No. DE-AC02-05CH11231.

P. Ferracin, S. E. Bartlett, S. Caspi , D. R. Dietderich, S. A. Gourlay, A. R. Hafalia, A. F. Lietzke, S. Mattafirri, A. D. McInturff, and G. L. Sabbi are with Lawrence Berkeley National Lab, Berkeley, CA 94720 USA (phone: 510-486-4630; fax: 510-486-5310; e-mail: pferracin@lbl.gov).

G. Ambrosio, B. Bordini, R. H. Carcagno, S. Feher, V. V. Kashikhin, M. J. Lamm, D. F. Orris, Y. M. Pischalnikov, C. D. Sylvester, M. A. Tartaglia, G. V. Velev, and A.V. Zlobin are with Fermilab National Accelerator Laboratory, Batavia, IL 60510-0500.

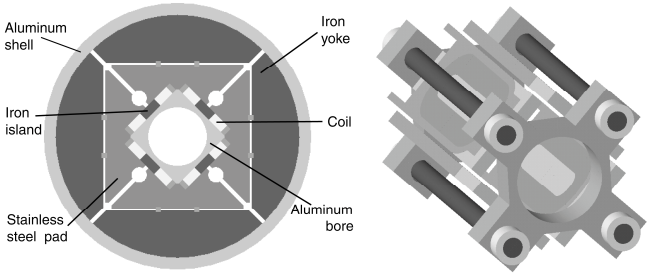

Fig. 1. SQ01 magnet cross-section (left) and longitudinal support (right).

II. Magnet Design

The design of the subscale quadrupole magnet (Fig. 1, left) consists of four "SC" type subscale coil modules: SC01 - SC02, previously successfully tested in several subscale dipole magnets, and SC15 - SC16, fabricated specifically for SQ01. The strands used in the cables of coil SC01 and SC02 were fabricated with the Modified Jelly Roll (MJR) process, while the strands for the new coils were formed by the Restacked Rod Process (RRP). Each SC module is a double-layer racetrack coil wound around an iron pole, reacted, and epoxy impregnated. The coil support structure, which comprises an aluminum bore, four stainless steel pads, four iron yokes, and an aluminum outer shell, was assembled with pressurized bladders and interference keys [7]. A longitudinal support system (Fig. 1, right), composed of four aluminum rods and two end plates, was used to reduce the conductor motion in the end region. A detailed description of the magnet structure, the assembly procedure, and the main parameters is given in [5].

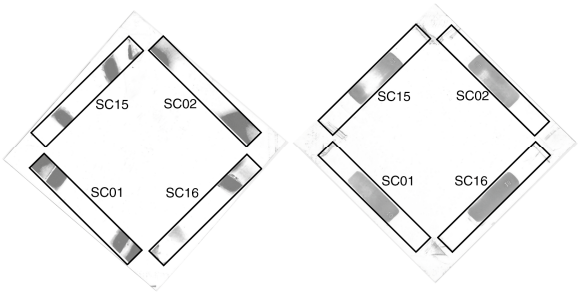

Fig. 2. Results of the pressure sensitive film test in the return end before (left) and after (right) the end load adjustments.

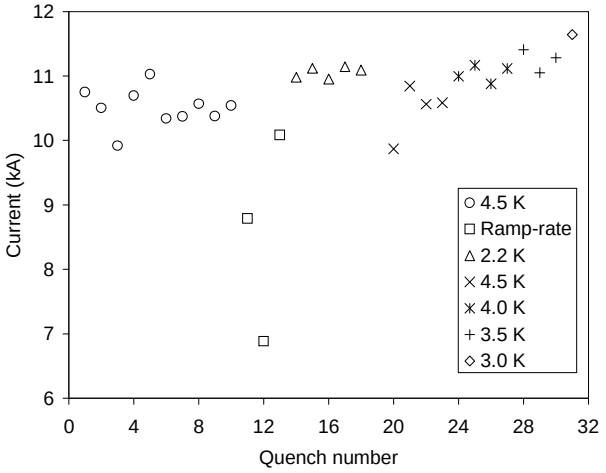

Fig. 3. SQ01b complete quench history.

III. Disassembly and Inspection

After the first test at LBNL, which indicated that the performance may have been limited by conductor movements, SQ01 was completely disassembled for visual inspection. Dimensional checks were conducted to look for pre-stress imbalances or non-uniformities, which may have caused the magnet quenches. After the axial rods were unloaded, pressure sensitive films were inserted between the end plates and the coils. These films indicated that the longitudinal force appeared to have been primarily applied on the sides of the coils (Fig. 2, left), and not in the middle, were the axial Lorentz forces were expected to be the largest. The results of 3D models predicted that, in order to minimize the conductor motion in the coil ends during excitation, the coil had to be supported at the center of the end region. Accordingly, shims were added to the end-plate, in a manner to center the end load over each coil (Fig. 2, right). Pressure sensitive films were also used to investigate coil pre-stress homogeneity in the azimuthal and radial directions. No significant pre-stress variations were observed on these coil surfaces. The magnet was then reassembled with the same room temperature level of pre-load as in SQ01 (i.e., 40 MPa and 90 MPa of tension respectively in shell and rods, corresponding to an expected coil straight section stress of 20 MPa at room temperature and 90 MPa at 4.5 K), and shipped to FNAL for testing as SQ01b.

IV. Test Results

Test of SQ01b (complete quench history shown in Fig. 3) included 10 training quenches at 4.5 K, 3 ramp-rate quenches,

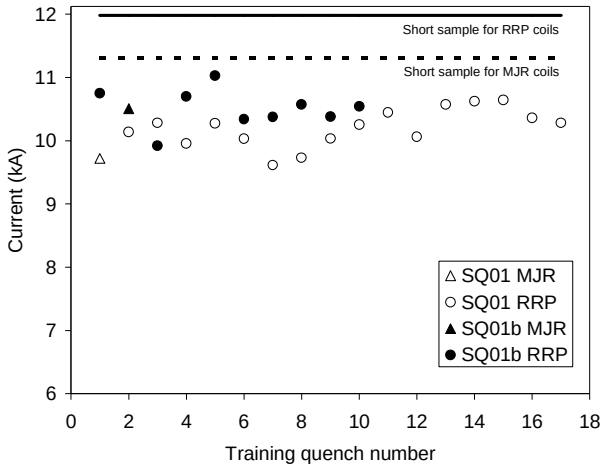

Fig. 4. 4.5 K training performance for SQ01 (white markers) and SQ01b (black markers); the round and triangle markers refer respectively to coils SC15-SC16 (RRP) and coils SC01-SC02 (MJR). The coil short sample expectations were computed from virgin strand measurements [5].

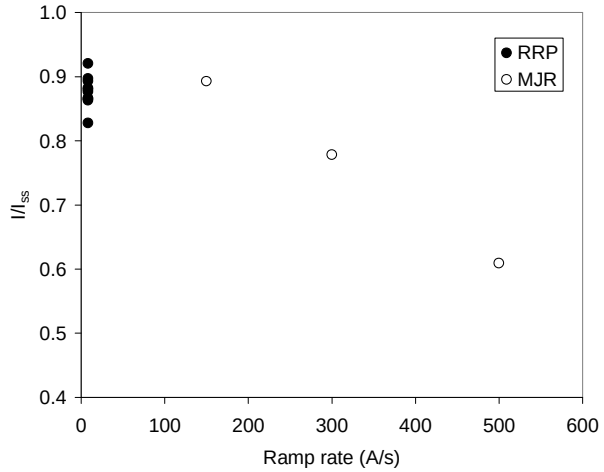

Fig 5. Ramp-rate dependence.

5 training quenches at 2.2 K, 4 additional 4.5 K training quenches, and several temperature-dependent quenches distributed in the 3.0-4.0 K range. Rotating coil magnetic measurements were performed, and the strains in the support structure and coils were monitored with strain gauges throughout the test. Attempts were also made to capture high-resolution voltage vs. time data of fast-flux disturbances and quench-onsets.

A. Training quenches

The current ramp profiles of SQ01b (40 A/s to 5000 A, 20 A/s to 8000 A, and 8 A/s to quench) were identical to those of SQ01, to facilitate the comparison between the two magnets. SQ01b's first training quench occurred at 10750 A (Fig 4), slightly above the SQ01's highest current observed at LBNL (10640 A). The highest training current (11030 A) was observed on the fifth attempt. Training was terminated after 10 quenches, when it exhibited an erratic plateau at similar currents as SQ01. Also similarly to SQ01, all but one training quench originated in the RRP coils. However, while SQ01's quenches originated in the high-field region of the coil (i.e. in the turns closest to the iron island), SQ01b's quench locations were predominantly in the outer section of the coil,

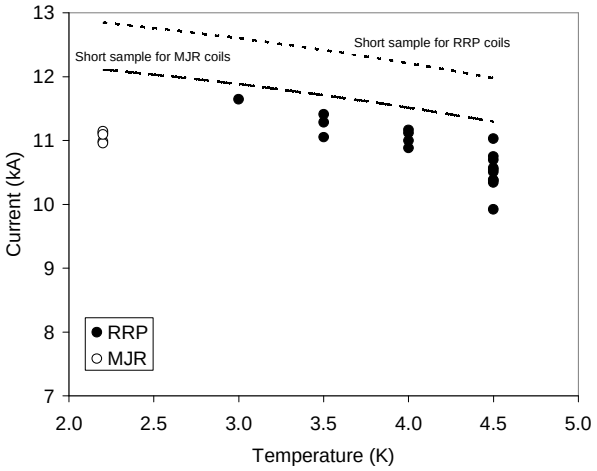

Fig. 6. Temperature dependence studies: quench data (markers) and short sample expectations for RRP and MJR coils as a function of temperature.

characterized by lower field. A detailed analysis of SQ01b's quench locations is presented in [8].

B. Ramp-rate dependence

Three ramp-rate quenches were performed at 500 A/s, 300 A/s, and 150 A/s. In Fig. 5 we plotted the fraction of quench current with respect to the coil short sample expectations (computed from virgin strand measurements), including the training quenches (8 A/s ramp-rate): all the ramp-rate quenches occurred in the MJR coils, with the 150 A/s value already within the band observed during training.

C. Temperature dependence studies

The magnet was subsequently cooled to determine its 2.2 K training performance (5 quenches, Fig. 3). Practically no increase of quench current was observed (the highest quench current was 11140 A), with a very stable plateau. However, the quench locations had moved from the RRP coils to the MJR coils. Training was then investigated in the 4.5-3.0 K temperature range (Fig. 6), in an attempt to estimate the conductor's temperature dependence, and to help localizing the temperature and current below which quenching originated in the MJR coils. The highest current (11640 A) was observed at 3.0 K, and all the quenches originated in the RRP coils. Fig. 6 also shows the relationship between these quenches and the extrapolated temperature dependence of the RRP virgin strand, showing that the offset observed at 4.5 K continues down to 3.0 K. We refer to [8] for further discussions on quench data.

D. Magnetic measurements

The rotating coil measurement system utilized a probe with an active length L_p of 250 mm, and a diameter of 25 mm. The measurements have been carried out positioning the center of the probe in three locations along the *z* axis, covering respectively the return end (- 250 mm to 0 mm), the magnet center (- 125 mm to + 125 mm), and the lead end (0 mm to + 250 mm). We point out that the coil straight section is 150 mm long, and the total coil length is 250 mm. In the transverse plane, the probe was centered using the "feed-down" technique of the quadrupole to dipole signal, and the coordinate system was oriented such that the skew quadrupole is zero. In Fig. 7

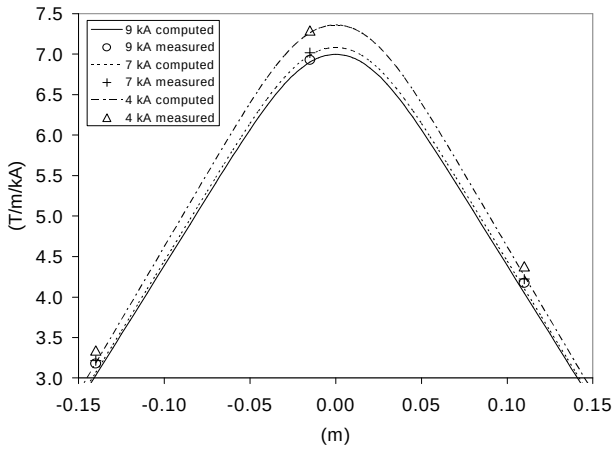

Fig. 7. Integrated transfer function (T/m/kA) at R_{ref} = 10 mm along a 250 mm probe as a function of the relative position (m) of the probe center with respect to the magnet center: meas. (markers) and computations (curves).

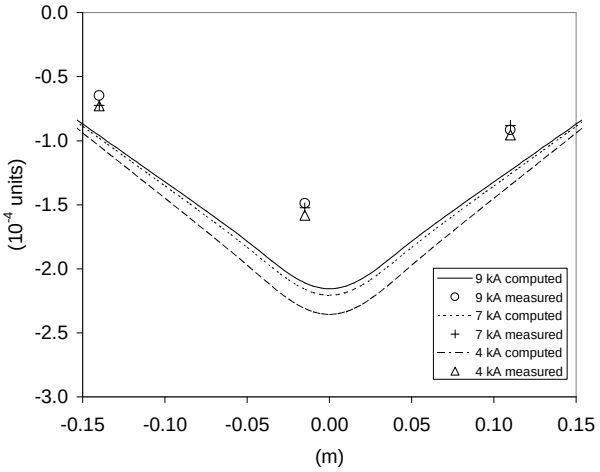

Fig. 8. Integrated b_6 (10^{-4} units) at R_{ref} = 10 mm along a 250 mm probe as a function of the relative position (m) of the probe center with respect to the magnet center: meas. (markers) and computations (curves).

and Fig 8 we plot respectively the transfer function (in T/m/kA) and the harmonic b_6 (in 10^{-4} units at a reference radius of 10 mm), both integrated along the probe length and measured after cool-down. The experimental data have been plotted for three different currents and as a function of the relative position of the probe center with respect to the magnet center. The b_6 was normalized by the main field component measured in the central position. With a correction of 15 mm to the *z* coordinates of the magnetic measurements, a good agreement between the measured and computed transfer function is obtained (Fig. 7). The integrated harmonics b_6 qualitatively agrees with the calculated dependence, exhibiting a positive offset of about 0.6 units (Fig. 8).

E. Strain gauge measurements

The magnet was instrumented with several strain gauges to measure the stress on the shell, on the aluminum rods, and on the RRP coils. The aluminum shell was instrumented with four half-bridge gauges measuring the azimuthal strain. The gauges were positioned at the four coil mid-planes in the axial center (z = 0), and all were equipped with temperature compensation gauges. Four additional full-bridge strain gauges were attached

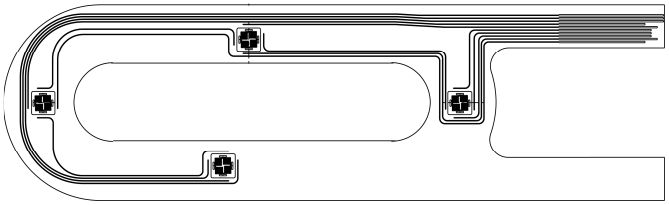

Fig. 9. Strain gauge location on coils SC15-SC16.

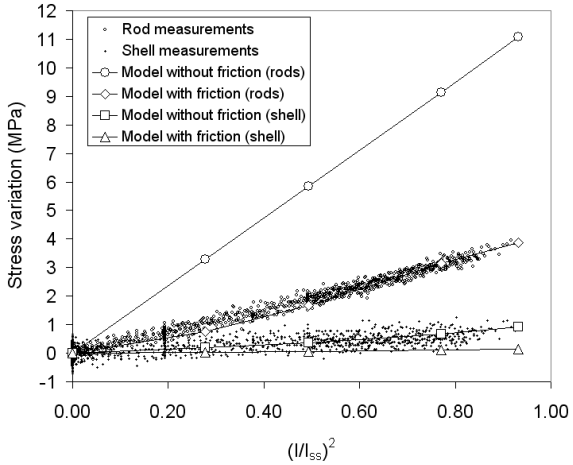

Fig. 10. Variation of tension in the shell and in the rods during magnet excitation as a function of the fraction of Lorentz force with respect to the 4.5 K short sample value.

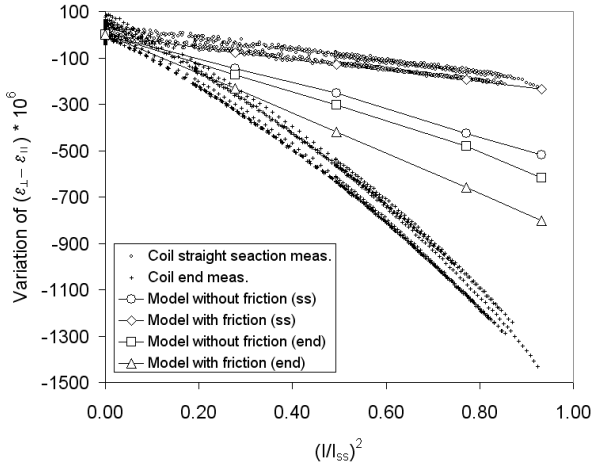

Fig. 11. Variation of bidirectional strain in the coil end regions during magnet excitation as a function of the fraction of Lorentz force with respect to the 4.5 K short sample value: $\varepsilon_\perp$ and $\varepsilon_{//}$ are respectively the strains perpendicular and parallel to the wide surface of the cable.

to the aluminum rods to measure their axial tension. Moreover, both RRP coils were instrumented with four full-bridge strain gauges placed directly over the turns and impregnated with them (Fig. 9). A coil trace overlay [9] was used to connect the strain gauges to the coils and to secure their position. Two gauges were located near the middle of the straight sections and two near the middle of the coil ends. The resulting signal was proportional to the difference between the turn-to-turn strain ($\varepsilon_\perp$), and the strain in the cable winding direction ($\varepsilon_{//}$).

In Fig. 10 the stress (tension) variations as a function of the fraction of Lorentz force with respect to the 4.5 K short sample value ($(I/I_{ss})^2$), both for the shell (in the azimuthal direction) and the rods (in the axial direction), are plotted. During excitation, the electromagnetic forces in the coil straight sections push the conductors toward the mid-planes, unloading the island pole, and producing an increase of azimuthal tension in the shell (within 1 MPa). In the end regions, the longitudinal Lorentz force tend to elongate the coils in the axial direction, thereby increasing the rods tension by about 4 MPa. As shown in Fig 10, the increase is well reproduced by the 3D finite element model predictions, as long as a friction factor μ = 0.1 between the coils and the components is included.

All coil strain gauges exhibited a decrease of the bidirectional strain ($\varepsilon_\perp$ - $\varepsilon_{//}$) both in the straight section and in the end regions (Fig. 11). The variation can be explained pointing out that the Lorentz forces tend to push outwardly the coil, i.e. separating it from the island pole. This effect determines, both on straight sections and ends, a turn-to-turn compression (negative $\varepsilon_\perp$) and a stretching in the coil winding direction (positive $\varepsilon_{//}$). As already observed in the rods, the results of the 3D model are in better agreement with the measurements when friction is included. In particular, the model reproduces the strain response of the coil straight section well, but it underestimates it at the coil ends.

V. Conclusions

The Nb_3Sn subscale quadrupole magnet SQ01 has been disassembled, visually inspected, reassembled, and retested as SQ01b after minor modifications in the end pre-load. The magnet performed similarly, achieving a slightly higher maximum current, compared to the first test. Ramp-rate and temperature dependence studies were conducted: at 2.2 K, a drop in quench current was observed in the MJR coils. Magnetic and strain gauges measurements were collected, analyzed and found consistent with numerical predictions.

VI. References

[1] A. Devred, S. A. Gourlay, and A. Yamamoto, "Future accelerator magnet needs", *IEEE Trans. Appl. Superconduct.*, Vol. 15, no. 2, pp. 1192-1199, June 2005.

[2] S. A. Gourlay. "Magnet R&D for the US LHC Accelerator Research Program", presented at *19th International Conference on Magnet Technology*, Genoa, Italy, September 18-23, 2005.

[3] R. C. Bossert, *et al.*, "Development of a 90-mm Nb_3Sn technological quadrupole for LHC upgrade based on SS collars", presented at *19th International Conference on Magnet Technology*, Genoa, Italy, September 18-23, 2005.

[4] S. Caspi, *et al.*, "Design and construction of TSQ01, a 90 mm Nb_3Sn quadrupole model for LHC luminosity upgrade based on a key and bladder structure", presented at *19th International Conference on Magnet Technology*, Genoa, Italy, September 18-23, 2005.

[5] P. Ferracin, *et al.*, "Development of a large aperture Nb_3Sn racetrack quadrupole magnet", *IEEE Trans. Appl. Superconduct.*, Vol. 15, no. 2, pp. 1132-1135, June 2005.

[6] B. Bordini, *et al.*, "SQ01b test summary", Fermilab Technical Division Note *TD-05-017*, January 2005.

[7] S. Caspi, *et al.*, "The use of pressurized bladders for stress control of superconducting magnets", *IEEE Trans. Appl. Superconduct.*, vol. 11, no. 1, pp. 2272-2275, March 2001.

[8] A. F. Lietzke, *et al.*, "Voltage Spike Observations in LARP Nb3Sn Coil Tests", presented at *19th International Conference on Magnet Technology*, Genoa, Italy, September 18-23, 2005.

[9] S. Caspi, *et al.*, "Measured strain of a Nb_3Sn coil during excitation and quench", *IEEE Trans. Appl. Superconduct.*, vol. 15, no. 2, pp. 1461-1464, June 2005.